

Negative hydrocarbon species $C_{2n}H^-$: How useful can they be?

Heng-Yong Nie^{a)}

Surface Science Western, The University of Western Ontario, 999 Collip Circle, London, Ontario N6G 0J3, Canada and Department of Physics and Astronomy, The University of Western Ontario, London, Ontario N6A 3K7, Canada

(Received 15 November 2015; accepted 29 January 2016; published 8 February 2016)

Time-of-flight secondary ion mass spectrometry (TOF-SIMS) analyzes chemical information by measuring ions generated via bombardment of an energetic ion beam on the surface of a specimen. Negative hydrocarbon ion species of $C_{2n}H^-$ are ubiquitous in TOF-SIMS for any hydrocarbon-containing materials, but their utilities are perhaps not fully explored. Using polyethylene, polypropylene, polyisoprene, and polystyrene, the author demonstrates that $C_{2n}H^-$ species possess intrinsic relationships, which offers unique TOF-SIMS ability for quantitatively differentiating the chemical structures of the four polymers. © 2016 American Vacuum Society.

[<http://dx.doi.org/10.1116/1.4941725>]

I. INTRODUCTION

Time-of-flight secondary ion mass spectrometry (TOF-SIMS)¹ is especially powerful in revealing chemical information on surface.^{2–10} In this technique, a pulsed (primary) ion beam is used to bombard the surface of a specimen to generate (secondary) ions from the topmost monolayer (1–3 nm), which are extracted, mass-separated, and detected in parallel, providing a powerful approach to detect chemicals on surface and understand surface chemistry. Because of the reactions of the impinging (primary) ions with organic surfaces,¹¹ TOF-SIMS provides extremely rich chemical information about organic materials, leading to possibilities of identifying chemicals. Extracting information to identify chemicals and explore their impact on surface chemistry is commonly described as data mining. If one can identify species that serve to reveal the structural information of the specimen under study, it is then possible to devise analytical approaches to explore surface chemistry and material structures.

For example, through identifying and making use of characteristic ion species, TOF-SIMS has been applied in examination of surface structures¹² of various polymers and cross-linking degrees^{13,14} of polymer films. Cross-linking degrees of ethyl lactate-based plasma polymer films have been examined by using the C/H ratio of an “average fragment” $C_xH_y^+$ calculated from principal component analysis of major positive hydrocarbon species (such as $C_2H_5^+$ and $C_3H_7^+$) for polymer films as a function of plasma power.¹³ Abmayr has presented positive secondary ion spectra for numerous polyolefin homo- and copolymers, showing that positive ion peak intensities (normalized to $C_2H_3^+$) can be used to differentiate polyolefins.¹⁵ During the early stages of TOF-SIMS, Briggs found that the peak intensity ratio of C^-/CH_2^- was sensitive to the degree of unsaturation of hydrocarbons, leading to a greater weighting in C_n clusters containing less hydrogen.^{16,17} It has been recently reported that the intensity ratio between negative hydrocarbon species C_6H^- and C_4H^- is capable of quantifying the cross-linking degrees of

poly(methyl methacrylate) (PMMA) films cross-linked using a surface-sensitive cross-linking technique, hyperthermal hydrogen projectiles induced cross-linking (HHIC).¹⁴ In this technique, a stream of kinetic hydrogen projectiles collides with the polymer surface and preferentially knocks off hydrogen atoms from the C–H bonds to generate carbon radicals leading to cross-linking of hydrocarbon chains.¹⁸

There are excellent recent reviews covering developments of TOF-SIMS instrumentation and applications,³ data interpretation, and the matrix effect,^{9,10} as well as determinations of surface structures¹² of polymers, from which there appear to be no reports on making use of $C_{2n}H^-$ in studying polymer structures. In this article, we demonstrate that there is an intrinsic relationship that exists between $C_{2n}H^-$ species, which can be used to quantitatively differentiate between the chemical structures of polyethylene (PE), polypropylene (PP), polyisoprene (PIP), and polystyrene (PS). The development of such a TOF-SIMS technique making use of $C_{2n}H^-$ species is expected to advance TOF-SIMS applications in exploration of surface chemistry and analytical chemistry.

II. EXPERIMENT

Low-density PE (Aldrich) with average $M_w \sim 35\,000$ and average $M_n \sim 7700$ was used to prepare thin films (~ 50 nm) by spin-coating a 1.5 wt. % PE solution in toluene onto a Si substrate. A thermally extruded, biaxially oriented PP film manufactured by 3M was used.¹⁹ A PIP sample was prepared by spreading *cis*-polyisoprene (liquid) made from synthetic rubber (Aldrich) on a clean aluminum foil. A PS sample was obtained by cutting a cross-section from a Dixie[®] 6 oz. PS foam cup (white colored).

An ION-TOF (Gmbh) TOF-SIMS IV equipped with a cluster bismuth liquid metal ion gun was employed to examine the four polymer samples. Five areas on each of the four polymer samples were analyzed. The base pressure of the analytical chamber was about 1×10^{-8} mbar. Unless otherwise specified, a pulse of 25 keV Bi_3^+ cluster primary ion beam (with a pulse width ~ 1 ns) was used to bombard the sample surface, at a fixed incident angle of 45° , to generate secondary ions. The secondary ions, either positive or

^{a)}Electronic mail: hnie@uwo.ca

negative at a time, were extracted by an electric field (2 kV) with an appropriate polarity. These ions with the same energy (2 keV) flew through a reflectron type of time-of-flight analyzer and arrived at the detector in times according to their masses. Their arrival times were converted to mass/charge ratio (m/z) via calibration of known species such as hydrogen, carbon, and hydrocarbons. Then, the sample surface was flooded with a pulsed, low energy (~ 18 eV) electron beam for neutralizing surface charging (the current was maintained below ~ 20 μA maximum to avoid sample damage). All these events triggered by one shot of the primary ion beam bombarding the sample surface were completed in a cycle time of 100 μs .

In our experiment, each spectrum was collected with 3×10^5 shots of the primary ion beam impinging on the sample surface over 128×128 pixels in an area of $300 \mu m \times 300 \mu m$. The target current generated by the pulsed primary ion beam was ~ 1 pA, resulting in ~ 600 ions per shot. Hence, the primary ion dosage was $\sim 2 \times 10^{11} \text{ cm}^{-2}$, which was within the conventional static limit of $1 \times 10^{13} \text{ cm}^{-2}$.²⁰ Poisson-correction was applied for the dead time effect of the detecting system.²¹ The negative secondary ion mass spectra were calibrated using H^- and C^- . The mass resolutions at C_2H^- and C_6H^- from spectra obtained on a polymer film were 3400 and 4800, respectively. For spectra obtained on the rather rough cross-section of the PS foam cup, the corresponding mass resolutions were degraded.

III. RESULTS AND DISCUSSION

Shown in Fig. 1 are negative secondary ion mass spectra obtained on samples of PE, PP, PIP, and PS in m/z 10–125. In order to make sure that the *cis*-PIP (liquid) spread on the aluminum foil stayed in vacuum of the TOF-SIMS analysis

chamber, we examined positive secondary ion mass spectra obtained on three areas (not shown). On the basis that no Al^+ was detected in the positive secondary ion mass spectra, we confirmed the formation of a PIP layer covering the aluminum foil. For all of the four polymers, hydrocarbon species of CH^- , C_2H^- , and C_4H^- are abundant, with C_2H^- being the most abundant. The spectrum for PIP shows that C_4H^- becomes more abundant in comparison with those for PE and PP. This trend of increased abundance of C_4H^- , C_6H^- , C_8H^- , and $C_{10}H^-$ relative to the most abundant C_2H^- becomes clearer for PS. Also shown in Fig. 1 are odd-numbered carbon chain species of C_3H^- , $C_3H_2^-$, C_5H^- , C_7H^- , and C_9H^- , whose intensities are much weaker in comparison with their adjacent even-numbered counterparts. In general, these negative hydrocarbon ion species are ubiquitous for any hydrocarbon-containing material.

Shown in Fig. 2 are ion intensities of C_2H^- , C_4H^- , C_6H^- , C_8H^- , and $C_{10}H^-$ normalized to the total ion intensity, which is a common way to compare abundances of ion species. The C_2H^- intensities for PE and PP are close to each other, both of which are more than 30% of the total ion intensity. For PIP, the C_2H^- intensity is slightly more than 25% of the total ion intensity. This ion intensity is approximately 20% for PS. The C_4H^- intensities for the four polymers are between 7% and 10% of the total ion intensity. The C_6H^- intensities for PE, PP, PIP, and PS increase monotonically from 1.4% to 3.9% with standard deviations less than 0.3%. This trend is also seen for C_8H^- and $C_{10}H^-$ ions, though their intensities decrease with increased carbon cluster sizes.

The spectra in Fig. 1 show various hydrocarbon species generated from the polymers and the $C_{2n}H^-$ intensities in Fig. 2 illustrate their abundances. However, are these spectra more useful than for just telling us what we already know,

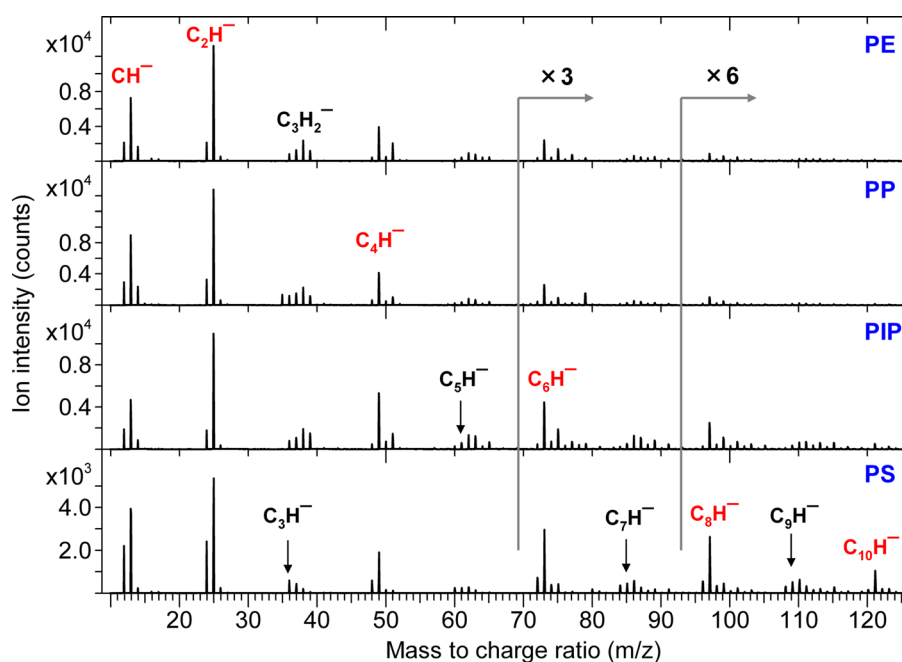


Fig. 1. (Color online) Negative secondary ion mass spectra obtained on PE, PP, PIP, and PS with the major hydrocarbon species indicated. The ion intensities are magnified three times from m/z 69 and six times from m/z 93 for clarity.

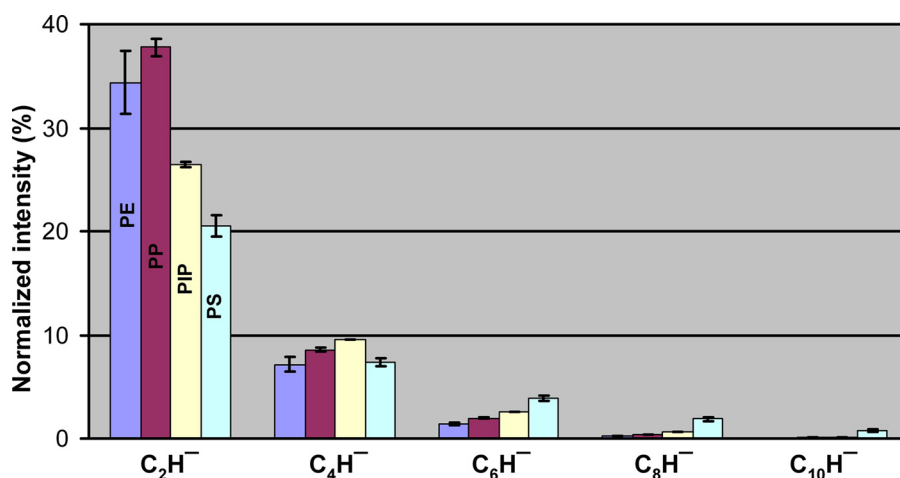


FIG. 2. (Color online) Ion intensities of C_2H^- , C_4H^- , C_6H^- , C_8H^- , and $C_{10}H^-$ normalized to the total ion intensity for PE, PP, PIP, and PS.

that they are made of hydrocarbons? Is there any way that we can extract more information from these spectra so that we can differentiate the four different polymers? For example, how can we tell PE from PP from their spectra that are quite similar to each other? In order to answer these demanding questions, we propose to use the intensity ratio between C_6H^- and C_4H^- , denoted as $\rho = C_6H^-/C_4H^-$, as a criterion to quantify differences among the four polymers. We have established in a previous report that the cross-linking degrees of PMMA films can be quantified by ρ .¹⁴ The PMMA films were cross-linked using the HHIC technique, in which hyperthermal hydrogen projectile knock out hydrogen atoms from two C–H bonds of adjacent hydrocarbon chains, leading to formation of a C–C bond between the two adjacent hydrocarbon chains.¹⁸ The cross-linking of hydrocarbon chains is thus essentially a hydrogen abstraction process that converts C–H bonds to C–C bonds. It is thus inferred that ρ perhaps provides clues on differentiating polymers by comparing their C–C bonds with C–H bonds.

In order to describe the structural differences among the four polymers, we define a parameter, coined as “carbon density” that counts, in principle, the degree of carbon atoms being bonded to other carbon atoms, rather than hydrogen atoms. Unsaturated hydrocarbons have a higher “carbon intensity” than saturated ones. Moreover, even without C=C double bonds, a carbon atom bonded to three or four other carbon atoms will also contribute to carbon density. As such, the carbon density introduced here mixes cross-linking and branching with double bonds. Further work to explore whether TOF-SIMS can differentiate between these two chemical structural features would require Fourier transform infrared spectroscopy, which is able to detect unsaturation and aromatic rings in the structure.²²

Illustrated in Fig. 3 are the chemical structures of monomers of PE, PP, PIP, and PS, with a formula of C_2H_4 , C_3H_6 , C_5H_8 , and C_8H_8 , respectively. Every carbon atom is bonded by C–C single bonds to other two carbon atoms in PE, while there are C=C double bonds in PS, which makes PE and PS have the lowest and highest carbon density, respectively, among the four polymers. In PP, there is one carbon atom

that is bonded to only one hydrogen atom, while in PIP, there is one double bond. In both PIP and PS, there is one carbon atom that is not bonded to any hydrogen atom. We infer that all carbon atoms that are not bonded to two hydrogen atoms contribute to increased carbon densities. The monomers of PE, PP, PIP, and PS illustrated in Fig. 3 are in the order of increasing carbon density as indicated by the insert arrow.

In order to gain new information on differentiating polymers with different chemical structures, we show in Fig. 4 the intensity ratios of C_2H^- , C_6H^- , C_8H^- , and $C_{10}H^-$ to C_4H^- . The C_2H^- intensity ratios decrease with increased carbon density for PE, PP, and PIP. For PIP and PS, however, the ratios are similar to each other. In order to determine whether it is the decrease in C_2H^- or increase in C_4H^- that makes a reduced C_2H^- intensity ratio, we look at the ion intensities of C_2H^- and C_4H^- normalized to total ion intensity (Fig. 2). For PE and PS, their C_4H^- intensities are quite similar to each other, while the C_2H^- intensity is much higher for PE than for PS. Therefore, for PE and PS, it can be said that C_2H^- is more easily formed from a polymer with a lower carbon intensity upon the primary ion beam bombardment in comparison with a polymer with a higher carbon density.

By contrast, the intensity ratios of longer chain species of C_6H^- , C_8H^- , and $C_{10}H^-$ increase with increased carbon densities. Specifically, the C_6H^- intensity ratio (i.e., ρ) for PE, PP, PIP, and PS are estimated to be $19.6 \pm 0.3\%$, $23.2 \pm 0.3\%$, $26.8 \pm 0.3\%$, and $52.9 \pm 1.6\%$, respectively.

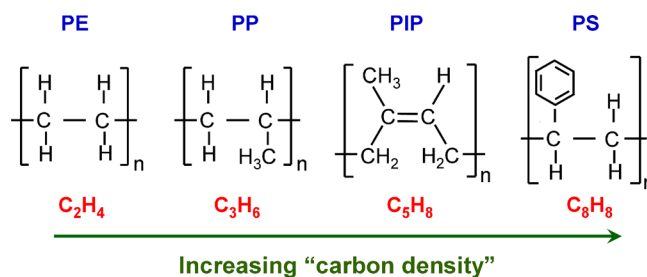


FIG. 3. (Color online) Illustration of the monomers of PE, PP, PIP, and PS in the order of increasing carbon density as described in text.

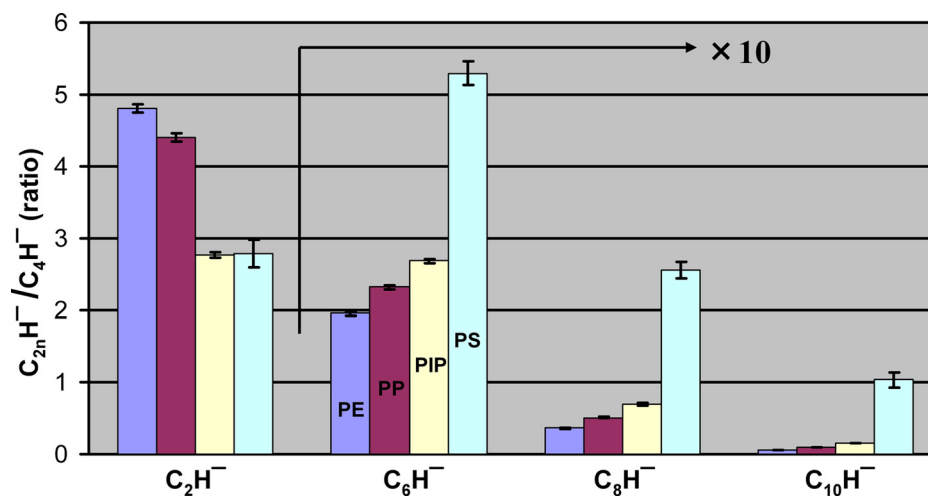


FIG. 4. (Color online) Intensity ratios of C_2H^- , C_6H^- , C_8H^- , and $C_{10}H^-$ to C_4H^- for PE, PP, PIP, and PS. The ratios of C_6H^- , C_8H^- , and $C_{10}H^-$ are magnified by ten times for clarity.

These numbers become $3.6 \pm 0.1\%$, $5.0 \pm 0.1\%$, $6.9 \pm 0.2\%$, and $25.6 \pm 1.2\%$ for the C_8H^- intensity ratios of the four polymers. For $C_{10}H^-$ species, the intensity ratios are less than 1% for PE and PP. Because the intensities of longer carbon chain species, especially $C_{10}H^-$ are rather weak for polymers with a low carbon density (e.g., PE, PP, and PIP), we select the intensity ratio of C_6H^- to C_4H^- (ρ) to quantify carbon density of the four polymers.

The repeatability of TOF-SIMS measurements on ρ was examined by comparing data collected on a PP film that we had used for several years as a clean substrate to support greasy or powdery substances for TOF-SIMS analyses. We checked this reference each time when we analyzed substances that had to be prepared on a substrate. The values of ρ for the PP film were $23.3 \pm 1.2\%$ from numerous spectra collected over the period of several years, proving that ρ is reproducible and thus can serve as a measure reflecting the chemical structure of the polymer. We stress that it is the intensity ratios of C_6H^- , C_8H^- , and $C_{10}H^-$ to C_4H^- , rather than their individual intensities, that are capable of differentiating polymers with different chemical structures.

From our experimental results shown in Fig. 4, we can draw two important conclusions about ρ : (1) each polymer has a specific ρ and (2) ρ increases with increased carbon densities. Therefore, ρ is capable of differentiating the four polymers, which suggests that C_6H^- and C_4H^- must have an intrinsic relationship that is dependent on the chemical structure of a polymer. This is vitally important to enrich our understanding of ion fragmentation of polymers and may provide clues to advancing analytical approaches based on TOF-SIMS.

It is interesting to note that many of the $C_{2n}H^-$ species we discussed also exist in interstellar media and in a DC discharge produced in laboratory through a flowing mixture of argon and acetylene at reduced pressures.^{23,24} Geometries and electronic structures of $C_{2n}H^-$ species have been investigated experimentally and theoretically in research areas of combustion and astrochemistry.^{25–29} Species of $C_{2n}H^-$ ($n = 2–4$) are known to be linear hydrocarbon species having

alternating single and triple bonds, with the carbon atom at one end bonded to a hydrogen atom and the one at the other end negatively charged via the capture of an electron.^{25–28} Knowledge from these research areas is useful for TOF-SIMS practitioners to better understand formation mechanisms and properties of $C_{2n}H^-$ species generated in TOF-SIMS. For example, as shown in Fig. 1, except for CH^- , odd-numbered carbon chain species of C_3H^- , C_5H^- , and C_7H^- have much lower intensities in comparison with even-numbered carbon chain species of C_2H^- , C_4H^- , C_6H^- , and C_8H^- . This TOF-SIMS observation can be explained by electronic configurations of the valence electrons that make the even-number species much more stable than the odd-numbered counterparts, resulting in binding energies of even-numbered $C_{2n}H^-$ (defined as the electron affinity of their neutral counterparts) that are significantly larger than those of odd-numbered $C_{2n+1}H^-$.²⁶

Because $C_{2n}H^-$ species detected in TOF-SIMS are apparently not structural entities in the polymers, they ought to form via combinations of multiple carbon atoms/ions and a single hydrogen atom/ion generated by the bombardment of the primary ions on the surface of polymers. Surprisingly, our TOF-SIMS results show that they have intrinsic relationships reflecting the chemical structures of polymers, strongly suggesting that the seemingly chaotic sputtering process perhaps contains more quantitative information about their chemical structures than we currently believe. This observation sheds insight into understanding ion fragmentation and developing potential TOF-SIMS analytical approaches, which is expected to expand applications of TOF-SIMS in polymer science and engineering. It has been more than two decades since Briggs pointed out that the relationship between the fragmented ions and the structure of hydrocarbons is a strong one.^{16,17} Our approach of using ρ to differentiate chemical structures of polymers is an important step forward toward understanding the relationship between $C_{2n}H^-$ and the chemical structures of polymers.

Since C_6H^- is used to calculate ρ , one should be cautious about other ions that may interfere with the intensity

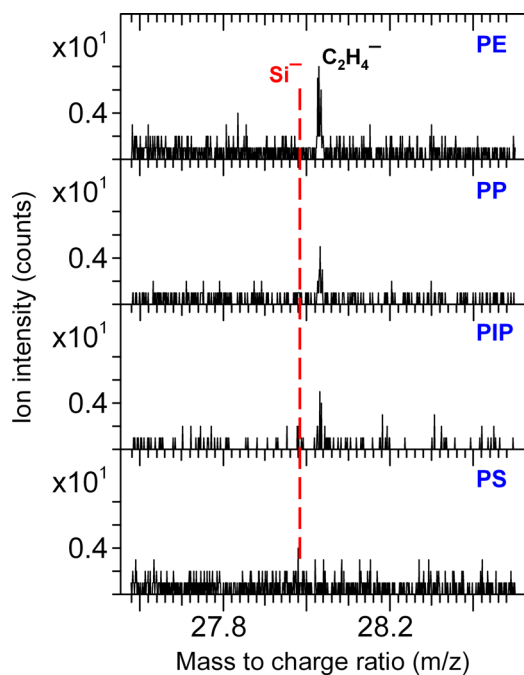


Fig. 5. (Color online) Negative secondary ion mass spectra of PE, PP, PIP, and PS showing the lack of Si^- on the surfaces of the four polymers, confirming that the polymers were free of siloxane.

estimation of C_6H^- . An obvious case is siloxane contamination that has a relatively abundant ion species $SiC_2H_5O^-$, which cannot be differentiated from C_6H^- because their m/z values (73.011 vs 73.008) are very close to each other. If a surface is contaminated with trace amounts of siloxane, it may not significantly increase the C_6H^- intensity. However, if the surface of a polymer film is contaminated by siloxane to the extent that the intensity C_6H^- be overestimated

significantly, one perhaps needs to make use of C_8H^- , which is not interfered with siloxane species. As shown in Fig. 5, no Si^- was detected on the surface of PE, PP, PIP, and PS we examined, confirming that there was no siloxane (a common surface contaminant) present on the four polymers. We also examined PMMA, an oxygen-containing polymer, and noticed a species of $C_3H_5O_2^-$ at m/z 73.029, which was weaker than C_6H^- at m/z 73.008. Therefore, for oxygen-containing polymers, $C_3H_5O_2^-$ would appear as a shoulder of the C_6H^- peak, which should be excluded when estimating the C_6H^- intensity.

The results shown above were obtained using a 25 keV Bi_3^+ primary ion beam. In order to illustrate the impact of primary ion beams on $C_{2n}H^-$, we collected secondary ion mass spectra on PE using 25 keV Bi^+ , Bi_3^{2+} , and Bi_5^+ , the other three primary ion beams generated from the same bismuth ion source of our instrument. The results are shown in Fig. 6, in which a spectrum obtained using Bi_3^+ is included for comparison purposes. The most striking shown in Fig. 6 is that the atomic bismuth ion Bi^+ generated a spectrum dominated by CH^- and C_2H^- ions. In comparison with the spectra obtained using cluster bismuth ions Bi_3^{2+} , Bi_3^+ , and Bi_5^+ , the intensity of C_4H^- obtained using Bi^+ is extremely weak, let alone those of C_6H^- , C_8H^- , and $C_{10}H^-$. This is in good agreement with previously reported results obtained using atomic primary ion beams, such as Ga^+ and Xe^+ : For aliphatic polymers, the negative ion mass spectra were dominated by CH^- and C_2H^- ions with little to no $C_{2n}H^-$ ions beyond C_4H^- , thus not useful in revealing the chemical structures of polymers.^{15–17}

As shown in Fig. 6, the spectra obtained using Bi_3^{2+} and Bi_3^+ are quite similar to each other, suggesting that it is the size of the cluster ion, rather than its amount of charge, that

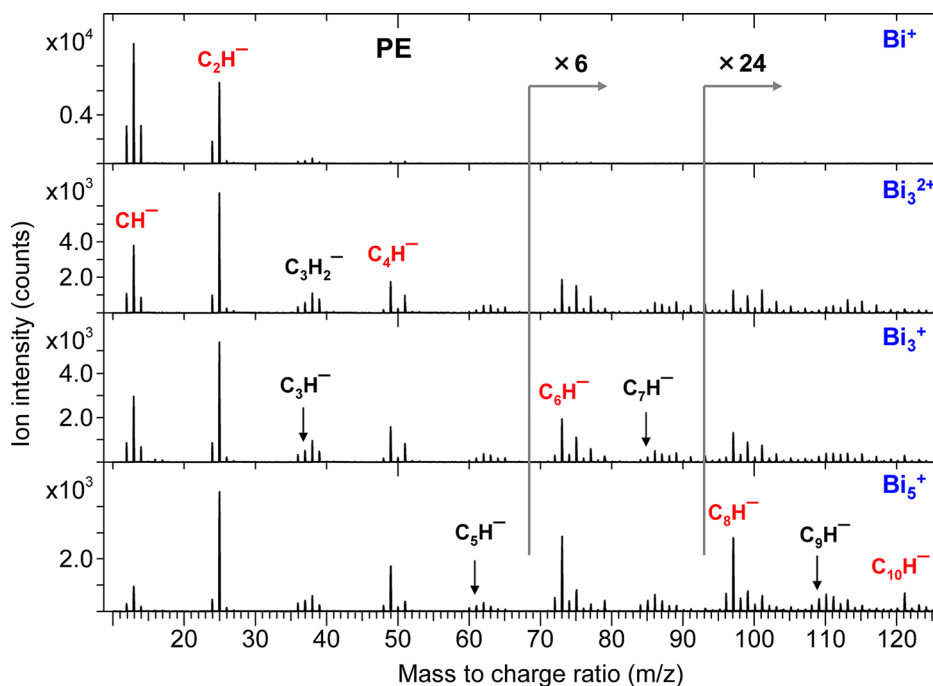


Fig. 6. (Color online) Negative secondary ion mass spectra obtained on PE using different primary ion beams of Bi^+ , Bi_3^{2+} , Bi_3^+ , and Bi_5^+ . The ion intensities are magnified six times from m/z 69 and 24 times from m/z 93 for clarity.

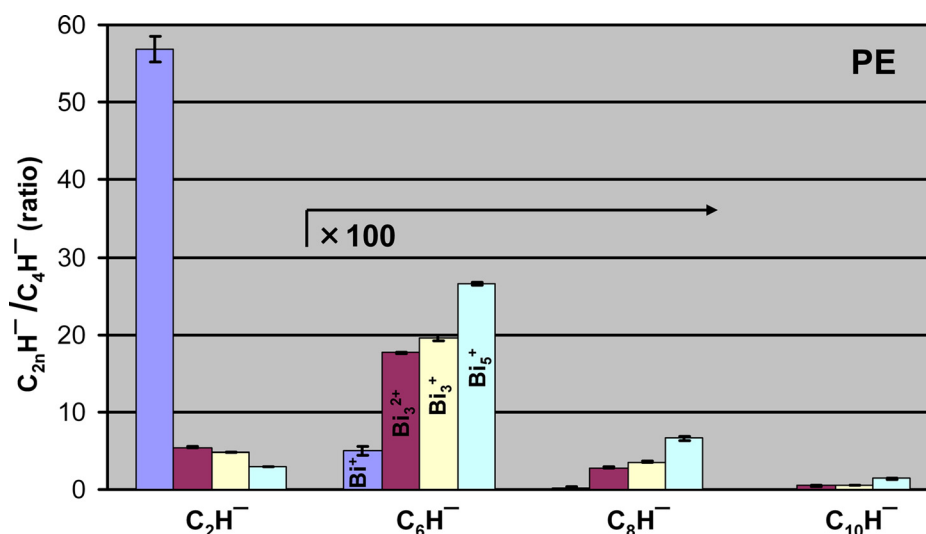


FIG. 7. (Color online) Intensity ratios of C_2H^- , C_6H^- , C_8H^- , and $C_{10}H^-$ to C_4H^- for PE using different primary ion beams of Bi^+ , Bi_3^{2+} , Bi_3^+ , and Bi_5^+ . The ratios of C_6H^- , C_8H^- , and $C_{10}H^-$ are magnified by 100 times for clarity.

plays the main role in fragmenting the polymer. C_6H^- , C_8H^- , and $C_{10}H^-$ appear to be more abundant in the spectra obtained using Bi_5^+ . This is another demonstration on that the ion yield of higher mass ion fragments characteristic to polymers can be enhanced significantly with the use of large cluster ion beams.⁴ It is interesting to note that CH^- has the highest intensity in the spectrum obtained using Bi^+ . The intensity of this ion reduces significantly in the spectra obtained using cluster bismuth ions. Its intensity becomes even weaker than that of C_4H^- in the spectrum obtained using Bi_5^+ .

In order to quantify how the four primary ion beams influence the relationship between $C_{2n}H^-$ ions, we show ion intensity ratios of $C_{2n}H^-$ to C_4H^- in Fig. 7. The C_2H^- ratio obtained using Bi^+ is extremely large, reaching 56.83 ± 1.72 , while this ratio reduces to 5.39 ± 0.09 , 4.81 ± 0.06 , and 2.88 ± 0.01 when using Bi_3^{2+} , Bi_3^+ , and Bi_5^+ , respectively. The C_6H^- ratio obtained using Bi^+ is as small as $5.0 \pm 0.5\%$, while the C_8H^- and $C_{10}H^-$ ratios are practically zero. The C_6H^- ratio obtained using Bi_3^{2+} is $17.7 \pm 0.1\%$, which is comparable to that obtained using Bi_3^+ ($19.6 \pm 0.3\%$). This ratio increases to $26.6 \pm 0.3\%$ when using Bi_5^+ . The C_8H^- ratio obtained using Bi_5^+ is $6.6 \pm 0.2\%$, a big jump from that obtained using Bi_3^+ ($3.6 \pm 0.1\%$). The $C_{10}H^-$ ratio obtained using Bi_5^+ reaches $1.4 \pm 0.1\%$, much larger than that obtained using Bi_3^+ ($0.6 \pm 0.1\%$).

We also examined ion mass spectra collected on the other three polymers (PP, PIP, and PS) using Bi_5^+ and confirmed that their intensity ratios of $C_{2n}H^-$ to C_4H^- follow the trend of those for PE (Fig. 7). For example, the C_6H^- ratios (i.e., ρ) obtained using Bi_5^+ for PP, PIP, and PS are $31.0 \pm 0.5\%$, $36.4 \pm 0.2\%$, and $60.6 \pm 2.1\%$, respectively, a fairly large increase from their counterparts obtained using Bi_3^+ that are $23.2 \pm 0.3\%$, $26.8 \pm 0.3\%$, and $52.9 \pm 1.6\%$, respectively. It is thus evident that the use of a larger bismuth cluster ion is beneficial in rendering higher intensity ratios of C_6H^- , C_8H^- , and $C_{10}H^-$ to C_4H^- . However, because the total ion intensity generated using Bi_5^+ is approximately half of that

generated using Bi_3^+ , we recommend the use of Bi_3^+ , unless in cases when measuring higher mass $C_{2n}H^-$ ions is the main interest.

IV. CONCLUSIONS

With the use of intensity ratios of $C_{2n}H^-$ relative to that of C_4H^- , we demonstrated that TOF-SIMS has the ability to differentiate between four polymers of PE, PP, PIP, and PS. The intensity ratio between C_6H^- and C_4H^- , denoted as $\rho = C_6H^-/C_4H^-$, is especially useful in qualifying differences among the four polymers. Specifically, with the use of cluster bismuth Bi_3^+ primary ion beam, ρ was estimated to be 20%, 23%, 27%, and 53% for PE, PP, PIP, and PS, respectively. Our experimental observations strongly suggest that intrinsic relationships exist among $C_{2n}H^-$ species. This finding is expected to enrich our understanding about chemical information carried by $C_{2n}H^-$ species that are generated from sputtering of organic materials by energetic primary ions. The demonstrated success of ρ in quantitatively differentiating the four polymers is expected to stimulate researchers involved in chemistry of materials and analytical chemistry to take advantage of this newly discovered TOF-SIMS ability to develop novel analytical approaches and explore surface chemistry.

ACKNOWLEDGMENTS

The author is grateful to Mary Jane Walzak for providing the polypropylene film used in this study and thanks to Surface Science Western and David Shoemith for their support of this work.

¹A. Benninghoven, *Angew. Chem. Int. Ed. Engl.* **33**, 1023 (1994).

²J. C. Vickerman and D. Briggs, *TOF-SIMS: Materials Analysis by Mass Spectrometry*, 2nd ed. (IM Publications LLP and SurfaceSpectra Ltd., Chichester, 2013).

³J. C. Vickerman and N. Winograd, *Int. J. Mass Spectrom.* **377**, 568 (2015).

⁴C. M. Mahoney, *Mass Spectrom. Rev.* **29**, 247 (2010).

- ⁵J. H. Wandass and J. A. Gardella, *J. Am. Chem. Soc.* **107**, 6192 (1985).
- ⁶A. Chilkoti, G. P. Lopez, B. D. Ratner, M. J. Hearn, and D. Briggs, *Macromolecules* **26**, 4825 (1993).
- ⁷A. M. Spool, *Surf. Interface Anal.* **36**, 264 (2004).
- ⁸H.-Y. Nie, *Anal. Chem.* **82**, 3371 (2010).
- ⁹A. V. Walker, *Anal. Chem.* **80**, 8865 (2008).
- ¹⁰A. G. Shard, S. J. Spencer, S. A. Smith, R. Havelund, and I. S. Gilmore, *Int. J. Mass Spectrom.* **377**, 599 (2015).
- ¹¹R. G. Cooks, T. Ast, and T. Pradeep, *Acc. Chem. Res.* **27**, 316 (1994).
- ¹²C.-M. Chan, L.-T. Weng, and Y.-T. R. Lau, *Rev. Anal. Chem.* **33**, 11 (2014).
- ¹³S. Ligot, E. Bousser, D. Cossement, J. Klemberg-Sapieha, P. Viville, P. Dubois, and R. Snyders, *Plasma Process. Polym.* **12**, 508 (2015).
- ¹⁴S. Naderi-Gohar, K. M. H. Huang, Y. L. Wu, W. M. Lau, and H.-Y. Nie, "A TOF-SIMS approach to probe cross-linking degree and depth of spin-coated poly(methyl methacrylate) films," *Polymer* (submitted).
- ¹⁵D. W. Abmayr, Jr., *Surf. Sci. Spectra* **13**, 117 (2006).
- ¹⁶D. Briggs, *Surface Analysis of Polymers by XPS and Static SIMS* (Cambridge University, Cambridge, 1988).
- ¹⁷D. Briggs, *Surf. Interface Anal.* **15**, 734 (1990).
- ¹⁸T. Trebicky *et al.*, *Green Chem.* **16**, 1316 (2014).
- ¹⁹H.-Y. Nie, M. J. Walzak, B. Berno, and N. S. McIntyre, *Appl. Surf. Sci.* **144-145**, 627 (1999).
- ²⁰J. S. Fletcher, N. P. Lockyer, S. Vaidyanathan, and J. C. Vickerman, *Anal. Chem.* **79**, 2199 (2007).
- ²¹T. Stephan, J. Zehnpenning, and A. Benninghoven, *J. Vac. Sci. Technol., A* **12**, 405 (1994).
- ²²J. Coates, "Interpretation of infrared spectra, a practical approach," in *Encyclopedia of Analytical Chemistry*, edited by R. A. Meyers (Wiley, Chichester, 2000).
- ²³M. C. McCarthy, C. A. Gottlieb, H. Gupta, and P. Thaddeus, *Astrophys. J.* **652**, L141 (2006).
- ²⁴S. Brunken, H. Gupta, C. A. Gottlieb, M. C. McCarthy, and P. Thaddeus, *Astrophys. J.* **664**, L43 (2007).
- ²⁵Y.-L. Sun, W.-J. Huang, and S.-H. Lee, *J. Chem. Phys. Lett.* **6**, 4117 (2015).
- ²⁶S. J. Blanksby, A. M. McAnoy, S. Dua, and J. H. Bowie, *Mon. Not. R. Astron. Soc.* **328**, 89 (2001).
- ²⁷L. Pan, B. K. Rao, A. K. Gupta, G. P. Das, and P. Ayyub, *J. Chem. Phys.* **119**, 7705 (2003).
- ²⁸M. Fehér and J. P. Maier, *Chem. Phys. Lett.* **227**, 371 (1994).
- ²⁹T. R. Taylor, C. S. Xu, and D. M. Neumark, *J. Chem. Phys.* **108**, 10018 (1998).